Article

Experimental and Theoretical Analysis of the Photochemistry and Thermal Reactivity of Ethyl Diazomalonate and Its Diazirino Isomer. The Role of Molecular Geometry in the Decomposition of Diazocarbonyl Compounds

Aneta Bogdanova, and Vladimir V. Popik

J. Am. Chem. Soc., **2004**, 126 (36), 11293-11302• DOI: 10.1021/ja047824r • Publication Date (Web): 20 August 2004

J|A|C|S
ARTICLES
Published on Web 08/20/2004

Experimental and Theoretical Analysis of the Photochemistry and Thermal Reactivity of Ethyl Diazomalonate and Its Diazirino Isomer. The Role of Molecular Geometry in the Decomposition of Diazocarbonyl Compounds

Aneta Bogdanova and Vladimir V. Popik*

Contribution from the Center for Photochemical Sciences, Bowling Green State University, Bowling Green, Ohio 43403

Received April 15, 2004; E-mail: vpopik@bgnet.bgsu.edu

Abstract: The photochemical or thermal decomposition of ethyl diazomalonate (**1**) or ethyl 3,3-diazirinedicarboxylate in methanol solutions yields the O−H insertion product **6**, while products of the Wolff rearrangement were not detected in both cases. The analysis of temperature-dependent ^{13}C NMR spectra and the results of DFT B3LYP/6-311+G(3df,2p) and MP2/aug-cc-pVTZ//B3LYP/6-311+G(3df,2p) calculations allow us to conclude that diazodiester **1** predominantly exists in the *Z*,*Z*-conformation. In contrast, photolysis of the cyclic isopropylidene diazomalonate (**3**), which also has a *Z*,*Z*-configuration of the diazodicarbonyl moiety, results in a clean Wolff rearrangement. These observations allow us to conclude that the direction of the photodecomposition of diazomalonates is not controlled by the ground-state conformation. The quantum-mechanical analysis of the potential energy surfaces for the dediazotization of **1** and **3** suggests that the formation of a carbene as a discrete intermediate is controlled by the ability of the latter to adopt a conformation in which carbonyl groups are almost orthogonal to the carbene plane. The outcome of the photolysis of ethyl diazomalonate depends on the wavelength of irradiation. Irradiation with 254 nm light results in the loss of nitrogen and the formation of dicarboethoxycarbene (**5**, $\Phi_{254} = 0.31$), while at longer wavelengths, diazirine **2** becomes an important byproduct ($\Phi_{350} = 0.09$). This observation suggests that the formation of carbene **5** and isomerization to diazirine proceed from different electronically excited states of ethyl diazomalonate.

Introduction

Photochemically or thermally induced extrusion of nitrogen from α-diazocarbonyl compounds usually leads to the formation of products formed by trapping of two different reactive intermediates, that is, ketenes and α-carbonylcarbenes (Scheme 1). Ketenes react with nucleophiles to produce carboxylic acid derivatives, and this overall process is known as the Wolff rearrangement.[1,2] α-Carbonylcarbenes, on the other hand, undergo an O−H or C−H insertion, add to π- bonds, or form ylides.[3]

The factors that direct the decomposition of α-diazocarbonyl compounds into a ketene or carbene pathway are still not well understood. It has been observed that cyclic diazoketones usually produce high or quantitative yields of ketenes, while in the case of their acyclic analogues, the Wolff rearrangement is often

Scheme 1

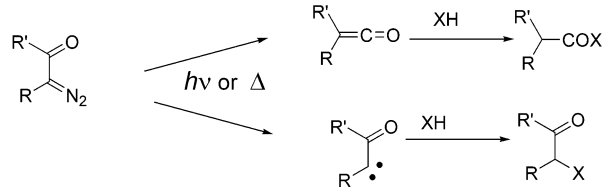

accompanied or even completely suppressed by carbene reactions.[4,5] The low-temperature NMR experiments unequivocally proved that α-diazocarbonyl compounds exist as an equilibrium of two conformations with *s*-*Z* and *s*-*E* arrangement of diazo and carbonyl groups.[6,7] The *s*-*Z* isomer usually predominates in the equilibrium, unless steric repulsions of substituents R and R′ destabilize it in favor of the *s*-*E* form.[1,8]

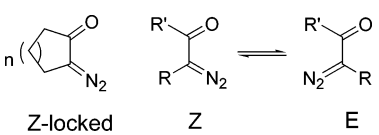

Based on the differences in the reactivity of 3,3,6,6-tetramethyl-2-diazocyclohexanone, which is locked in the *s*-*Z* configuration, and 2,2,5,5-tetramethyl-4-diazo-3-hexanone,[5,9] which is forced to adopt the *s*-*E* conformation by bulky *tert*-butyl substituents, Kaplan postulated that *s*-*Z* conformers of

(1) Kirmse, W. *Eur. J. Org. Chem.* **2002**, 2193.
(2) Meier, H.; Zeller, K.-P. *Angew. Chem., Int. Ed. Engl.* **1975**, *14*, 32. (b) Regitz, M.; Maas, G. *Diazo Compounds*; Academic Press: Orlando, FL, 1986. (c) Ye, T.; McKervey, A. M. *Chem. Rev.* **1994**, *94*, 1091. (d) Doyle, M. P.; McKervey, M. A.; Ye, T. *Modern Catalytic Methods for Organic Synthesis with Diazo Compounds*; Wiley-Interscience: New York, 1998; pp 487−534. (e) Zeller, K.-P.; Meier, H.; Muller, E. *Tetrahedron* **1972**, *28*, 5831.
(3) Toscano, J. P. In *Advances in Carbene Chemistry*; Brinker, U. H., Ed.; JAI Press: Greenwich, CT, 1998; Vol. 2, pp 216−245. (b) Jones, M.; Moss, R. A. *Carbenes*; Wiley: New York, 1973. (c) Zollinger, H. *Diazo chemistry, 2. Aliphatic, inorganic, and organometallic compounds*; VCH Publishers: New York, 1995; pp 305−357. (d) Kirmse, W. Carbenes and the O−H bond. In *Advances in Carbene Chemistry*; Brinker, U. H., Ed.; JAI Press Inc.: Greenwich, CT, 1994; pp 1−57. (e) Miller, D. J.; Moody, C. J. *Tetrahedron* **1995**, *40*, 10811.

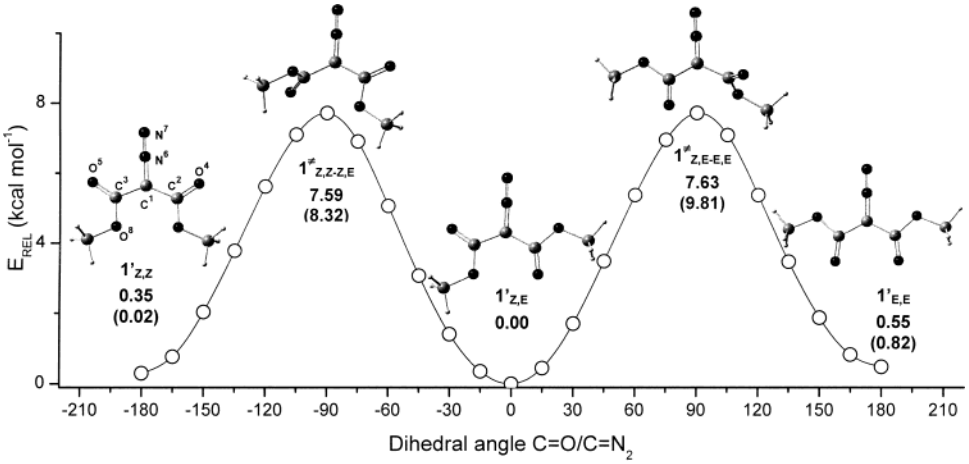

Figure 1. Conformational energy profile for methyl diazomalonate (**1′**) obtained using the relaxed scan of PES at the B3LYP/6-31+G(d,p) level. The geometries of three stable conformations of methyl diazomalonate (**1′**) and the transition states for the rotation around CO−CN_2 bonds (**1**‡) were optimized at the B3LYP/6-311+G(3df,2p) level of theory.

α-diazocarbonyl compounds undergo a concerted Wolff rearrangement to ketenes, whereas the *s-E* form loses nitrogen to produce α-carbonylcarbene. The latter can undergo isomerization into ketenes or be trapped by external reagents. While this hypothesis has been adopted by other authors,[3a,10] some established *s-E* diazo ketones produce ketenes with ease.[11]

One of the most impressive examples of the structural control of the Wolff rearrangement is found in the family of diazomalonic acid esters. Cyclic isopropylidene diazomalonate (diazo Meldrum's acid, **3**) undergoes an efficient Wolff rearrangement both thermally[12] and photochemically,[12,13] while acyclic diazomalonates, such as **1**, produce only carbenic products in solution.[14,15] The conventional explanation for this phenomenon is based on the assumption that the irradiation of conformationally flexible acyclic α-diazoesters produces carbalkoxycarbenes, which do not rearrange due to the low migratory aptitude of oxygen.[2a] The excitation of *Z,Z*-locked diazo Meldrum's acid, on the other hand, results in the concerted Wolff rearrangement that bypasses the α-carbonyl carbene step.

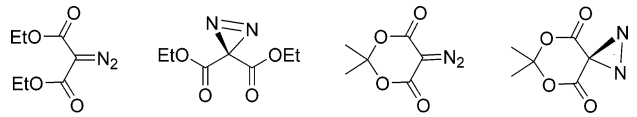

1 **2** **3** **4**

We have recently reported experimental and theoretical evidence supporting the concerted mechanism for the Wolff rearrangement of the diazo Meldrum's acid. However, the corresponding α,α′-dicarbonylcarbene, which is apparently produced in the photolysis of diazirine **4**, smoothly rearranges to ketene with virtually no activation barrier.[12] To get a better understanding of the structural influence on the reactivity of α-diazocarbonyl compounds, we undertook a detailed investigation of the photo- and thermal chemistry of conformationally flexible acyclic ethyl diazomalonate (**1**) and the corresponding diazirine **2**.

Results and Discussion

Conformational Analysis. The DFT/MP2 analysis of the structure and reactivity of ethyl diazomalonate (**1**) was conducted on the example of methyl diazomalonate (**1′**, Figure 1). Ethyl groups in **1′** were replaced with methyl groups to simplify calculations. In our opinion, this modification should not significantly disturb the relative energies of the species involved in the transformations of **1**.

There are three relatively stable conformations of the α-diazo-β,β-dicarbonyl fragment in acyclic diazomalonates: *Z,Z*; *Z,E*;

(4) Horner, L.; Korobitsyna, I. K.; Rodina, L. L.; Sushko, T. P. *Zh. Org. Khim.* **1968**, *4*, 175. Timm, U.; Zeller, K. P.; Meier, H. *Tetrahedron* **1977**, *33*, 453. Tomioka, H.; Okuno, H.; Izawa, Y. *J. Org. Chem.* **1980**, *45*, 5278. Rau, H.; Bokel, M. *J. Photochem. Photobiol., A* **1990**, *53*, 311. Hadel, L. M.; Maloney, V. M.; Platz, M. S.; McGimpsey, W. G.; Scaiano, J. C. *J. Phys. Chem.* **1986**, *90*, 2488. Tomioka, H.; Hirai, K.; Tabayashi, K.; Murata, S. *J. Am. Chem. Soc.* **1990**, *112*, 7692. Chiang, Y.; Kresge, A. J.; Pruszynski, P.; Schepp, N. P.; Wirz, J. *Angew. Chem., Int. Ed. Engl.* **1991**, *30*, 1366. Charette, A. B.; Wurz, R. P.; Ollevier, T. *Helv. Chim. Acta* **2002**, *85*, 4468. Tippmann, E.; Holinga, G.; Platz, M. S. *Org. Lett.* **2003**, *5*, in press.
(5) Kaplan, F.; Mitchell, M. L. *Tetrahedron Lett.* **1979**, *9*, 759.
(6) Kaplan, F.; Meloy, G. K. *Tetrahedron Lett.* **1964**, 2427. Kaplan, F.; Meloy, G. K. *J. Am. Chem. Soc.* **1966**, *88*, 950. Kessler, H.; Rosenthal, D. *Tetrahedron Lett.* **1973**, 393. Curci, R.; DiFuria, F.; Lucchini, V. *Spectrosc. Lett.* **1974**, *7*, 211. Lichter, R. L.; Srinivasan, P. R.; Smith, A. B., III; Dieter, R. K.; Denny, C. T. *Chem. Commun.* **1977**, 366. Dickert, F. L.; Soliman, F. M.; Bestmann, H. J. *Tetrahedron Lett.* **1982**, *23*, 2639.
(7) Nikolaev, V. A.; Rodina, L. L.; Korobitsyna, I. K. *Zh. Org. Khim.* **1974**, *10*, 1555. (b) Lauer, W.; Krause, V.; Wengenroth, H.; Meier, H. *Chem. Ber.* **1988**, *121*, 465. (c) Nikolaev, V. A.; Popik, V. V. *Zh. Org. Khim.* **1989**, *25*, 1014.
(8) Sorriso, S. In *The Chemistry of Diazonium and Diazo Groups*; Patai, S., Ed.; Wiley: Chichester, 1978; pp 95−136. Goodman, J. M.; James, J. J.; Whiting, A. *J. Chem. Soc., Perkin Trans. 2* **1994**, 109.
(9) Geometry optimization of this diazo compound, that we conducted at the b3lyp/6-311+G(3df,2p) level of theory, produced the planar *s-E* conformation.
(10) Tomioka, H.; Okuno, H.; Izawa, Y. *J. Org. Chem.* **1980**, *45*, 5278. Tomioka, H.; Kondo, M.; Izawa, Y. *J. Org. Chem.* **1981**, *46*, 1090. Marfisi, C.; Verlaque, P.; Davidovics, G.; Pourcin, J.; Pizzala, L.; Aycard, J.-P.; Bodot, H. *J. Org. Chem.* **1983**, *48*, 533. Tsuda, M.; Oikawa, S.; Nagayama, K. *Chem. Pharm. Bull.* **1987**, *35*, 1. Tsuda, M.; Oikawa, S. *Chem. Pharm. Bull.* **1989**, *37*, 573. Torres, M.; Gosavi, R. K.; Lown, E. M.; Piotrkowski, E. J.; Kim, B.; Bourdelande, J. L.; Font, J.; Strausz, O. P. *Stud. Phys. Theor. Chem.* **1992**, *77*, 184. Toscano, J. P.; Platz, M. S.; Nikolaev, V.; Popik, V. *J. Am. Chem. Soc.* **1994**, *116*, 8146.
(11) Zeller, K. P. *Chem. Ber.* **1979**, *112*, 678. Fenwick, J.; Frater, G.; Ogi, K.; Strausz, O. P. *J. Am. Chem. Soc.* **1973**, *95*, 124. Torres, M.; Ribo, J.; Clement, A.; Strausz, O. P. *Can. J. Chem.* **1983**, *61*, 996.
(12) Bogdanova, A.; Popik, V. V. *J. Am. Chem. Soc.* **2003**, *125*, 14153.
(13) Nikolaev, V. A.; Khimich, N. N.; Korobitsyna, I. K. *Khim. Geterotsikl. Soedin.* **1985**, 321. Lippert, T.; Koskelo, A.; Stoutland, P. O. *J. Am. Chem. Soc.* **1996**, *118*, 1551. Winnik, M. A.; Wang, F.; Nivaggioli, T.; Hruska, Z.; Fukumura, H.; Masuhara, H. *J. Am. Chem. Soc.* **1991**, *113*, 9702. Stevens, R. V.; Bisacchi, G. S.; Goldsmith, L.; Strouse, C. E. *J. Org. Chem.* **1980**, *45*, 2708. Kammula, S. L.; Tracer, H. L.; Shelvin, P. B.; Jones, M., Jr. *J. Org. Chem.* **1977**, *42*, 2931.
(14) Wang, J.-L.; Toscano, J. P.; Platz, M. S.; Nikolaev, V.; Popik, V. *J. Am. Chem. Soc.* **1995**, *117*, 5477. (b) Jones, M., Jr.; Ando, W.; Hendrick, M. E.; Kulczucki, A.; Howley, P. M.; Hummel, K. F.; Malament, D. S. *J. Am. Chem. Soc.* **1972**, *94*, 7469.
(15) In the absence of trapping reagent, for example, in cryogenic matrix or in the gas phase, dicarbalkoxycarbene can undergo Wolff rearrangement: Visser, P.; Zuhse, R.; Wong, M. W.; Wentrup, C. *J. Am. Chem. Soc.* **1996**, *118*, 12598.

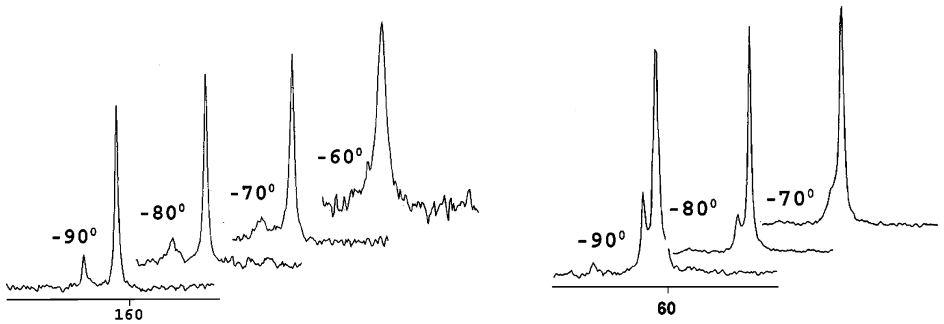

Figure 2. Temperature-dependent ^{13}C spectra of diethyl diazomalonate.

Table 1. Relative Energies and Main Geometrical Parameters of the Equilibrium and Transition Structures Obtained at the B3LYP/6-311+G(3df,2p)//B3LYP/6-311+G(3df,2p) and MP2 (full) aug-cc-pVTZ//B3LYP/6-311+G(3df,2p) (in Parentheses) Levels

	$1'_{ZZ}$	$1'_{ZE}$	$1'_{EE}$	$1^{\ddagger}_{ZZ\rightarrow ZE}$	$1^{\ddagger}_{ZE\rightarrow EE}$	2′
E_{rel}[a]	0.35	0.00	0.55	7.59	7.63	24.17
ZPVE corrected (kcal/mol)	(0.02)		(0.82)	(8.32)	(9.81)	(20.73)
C^1-N^6 distance[b]/Å	1.326	1.322	1.318	1.302	1.301	1.506
N^6-N^7 distance/Å	1.110	1.110	1.110	1.120	1.120	1.200
-∠$C^2C^1C^3$/deg	134.5	129.6	124.9	124.7	120.7	124.5
-∠$C^3C^1C^2O^4$/deg	180.0	180.0	0.0	−87.6	−3.5	−12.7
-∠$C^2C^1C^3O^5$/deg	180.0	0.0	0.0	177.1	−86.4	162.9

[a] Energy difference between $\mathbf{1'_{Z,E}}$ and the corresponding structure. [b] The numbering of atoms in structures **1′**, $\mathbf{1^{\ddagger}}$, and **2′** is shown in Figure 1.

and *E*,*E*. The DFT optimized geometry of these conformers, as well as the geometries of the transition states for *Z*,*Z* → *Z*,*E* and *Z*,*E* → *E*,*E* interconversions, are shown in Figure 1. The electronic energies and representative structural parameters of these structures, as well as those of dimethyl 3,3-diazirinedicarboxylate (**2′**), are summarized in Table 1. Energies shown in the text and in the figures correspond to B3LYP/6-311+G(3df,2p) calculations, while values in parentheses were obtained using the MP2(full)/aug-cc-pVTZ//B3LYP/6-311+G(3df,2p) method. It is interesting to note that all three conformers were calculated to be perfectly planar, which indicates the absence of substantial steric interactions. The *E*,*E*-conformer is predicted to be the least stable one, while *Z*,*Z* and *Z*,*E* have similar energies. The preference for the *Z*-arrangement of diazo and carbonyl functionalities is usually explained by the Coulombic attraction between the positively charged nitrogen of the diazo group and the negatively charged carbonyl oxygen atom.[8] The barrier for the interconversion between conformations was predicted to be in the range of 7.6−9.8 kcal/mol (Table 1). In the transition state from *Z*,*Z* to *Z*,*E*, as well as for the *Z*,*E* to *E*,*E* transformation, the carbonyl group that has the same arrangement in both conformers stays virtually coplanar with the diazo group, while the other carbonyl fragment is almost orthogonal to the C═N_2 plane.[16] The conformational energy profile shown in Figure 1 was obtained by conducting a relaxed scan of the potential energy surface starting from the *Z*,*E*-conformer and following the dihedral angle between diazo and one of the carbonyl groups.

Low-temperature NMR experiments allowed us to observe the conformational equilibrium of ethyl diazomalonate in solutions. At room temperature, the ^{13}C spectrum of **1** contains only one set of signals for all carbons. At ca. −30 °C, the signal of the carbonyl group becomes broad and splits in two below −60 °C (Figure 2).

Similar changes are observed in the methylene region of the spectrum, where splitting of the signal is observed below −70 °C. The coalescence temperature for the carbonyl signals, T_{coal} = −60 °C, and for methylene signals, T_{coal} = −70 °C, allows us to evaluate the barrier for the conformational interconversion. For both temperatures, we have obtained identical values of activation energy $\Delta G^{\ddagger}_{213K} = \Delta G^{\ddagger}_{203K} = 9.3$ kcal/mol, which are in a good agreement with DFT/MP2 results (Table 1). From the shape of the NMR signals observed at conditions of slow exchange (Figure 2), we can conclude that diethyl diazomalonate exists in solution as a rapid equilibrium of two conformations. The major conformer, ca. 85%, should be a symmetrical one as it has only one set of signals in the ^{13}C spectrum. Quantum-mechanical calculation (vide supra), as well as the known predominance of the *Z*,*Z*-conformer in sterically unhindered 2-diazo-1,3-diketones,[7] allows us to assign *Z*,*Z*-structure to this conformer. The alternative symmetrical conformation, *E*,*E*, is predicted to be higher in energy than *Z*,*Z* and *Z*,*E* by all quantum-mechanical models, from semiempirical AM1 to density functional b3lyp and to correlative MP2. In fact, the *E*,*E*-conformer was observed only as a minor component of the equilibrium mixture in diazodicarbonyl compounds with bulky substituents.[7,17] Additional support for this assignment comes from the fact that the carbonyl signal of the *s*-*E* carbonyl group in diazodicarbonyl compounds is usually observed at lower fields than the *s*-*Z* signal.[7,17] The assignment of a minor component is more difficult. The signal at 163.25 ppm can represent both carbonyl groups of a symmetrical *E*,*E*-conformation or *E*-fragment of the *Z*,*E*-conformer, while signals of the *Z*-part overlap with an intense peak of the major *Z*,*Z*-form. On the basis of the experimental and theoretical results discussed above, we favor *Z*,*E*-assignment.

In the diazirine **2**, the central carbon atom (**C^1**) is formally sp^3 hybridized, and rotation of the carbonyl fragments around

(16) The optimized geometries for the species discussed in the paper are provided in the Supporting Information.

(17) Nikolaev, V. A.; Popik, V. V.; Korobitsyna, I. K. *Zh. Org. Khim.* **1991**, *27*, 505.

C(=O)−C[1] should be virtually free. In fact, DFT calculations predict the barrier for such a rotation in **2′** to be in the order of 2 kcal/mol. The conformational analysis found three relatively stable rotamers, which are very close in energy: $\Delta\Delta E°$ values are 0 and 1.1 kcal/mol correspondingly. The geometrical parameters for the rotamer with the lowest energy are shown in Table 1.[16] In other words, irradiation of **2** should result in the excitation of a broad spectrum of ground-state conformations.

Thermal Reactions of the Ethyl Diazomalonate (1) and Ethyl 3,3-Diazirinedicarboxylate (2). Diazomalonate (**1**) is a relatively stable compound; for example, virtually no decomposition was observed in aqueous or methanolic solutions at 80 °C for 24 h. Due to the high stability of this diazo compound, little is known about products resulting from its thermal decomposition. We found that heating ethyl diazomalonate (**1**) at 150 °C in neat methanol for 6 h results in quantitative formation of ethyl 2-methoxymalonate (**6**), the apparent product of carbene **5** insertion into the O−H bond of a solvent (Scheme 2). The latter was independently prepared by rhodium-catalyzed decomposition of ethyl diazomalonate in the presence of methanol (see Experimental Section). Formation of the insertion product in the thermolysis of **1** is in sharp contrast with the thermolysis of cyclic analogue **3**, which produces only Wolff rearrangement products.

Scheme 2

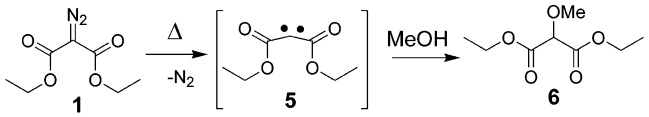

The isomeric diethyl 3,3-diazirinedicarboxylate (**2**), on the other hand, is rather labile and undergoes slow decomposition even at room temperature with $k_{25°C} = (3.7 \pm 0.3)*10^{-5}$ s^{-1} in methanol. Mild heating of **2** in a methanol solution results in the rapid decomposition and formation of the O−H insertion product **6**. The isomerization into the diazo compound, which is the only process observed in the case of cyclic diazirine **4**,[12] produced only trace amounts (ca. 2%) of ethyl diazomalonate (**1**, Scheme 3).

Scheme 3

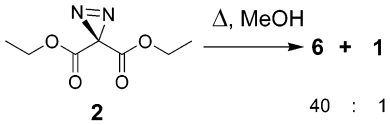

Rates of the decomposition of diazirine **2** were measured in aqueous and dioxane solutions in the temperature range from 30 to 70 °C. The progress of the reaction was followed by the decrease in absorbance of **2** at 291 nm. The data so obtained are summarized in Tables S1−S2 and are displayed as a temperature rate profile in Figure 3.

The decomposition of **2** is 2−4 times faster in water than in dioxane, and this rate difference increases with temperature, indicating a substantial difference in the entropy of activation. In fact, least-squares fitting of the data gives the following activation parameters: $\Delta H^{‡} = 24.9 \pm 0.6$ kcal M^{-1} and $\Delta S^{‡} = 2.8 \pm 1.6$ cal M^{-1} K^{-1} in aqueous solutions; and $\Delta H^{‡} = 22.2 \pm 0.6$ kcal M^{-1} and $\Delta S^{‡} = -7.4 \pm 1.8$ cal M^{-1} K^{-1} in dioxane.

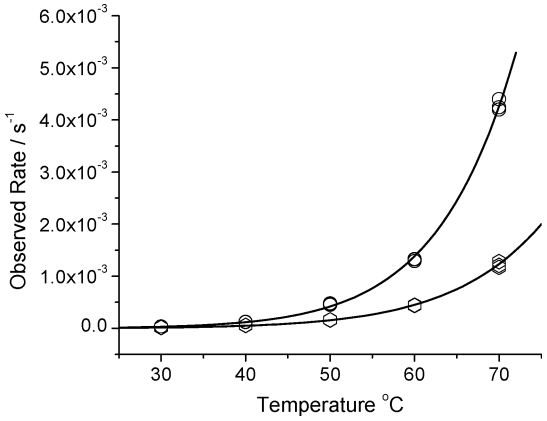

Figure 3. Temperature rate profiles for the decomposition of diazirine **2** in aqueous (circles) and dioxane (hexagons) solutions. The lines shown were drawn using parameters obtained by least-squares fitting of the Eyring equation.

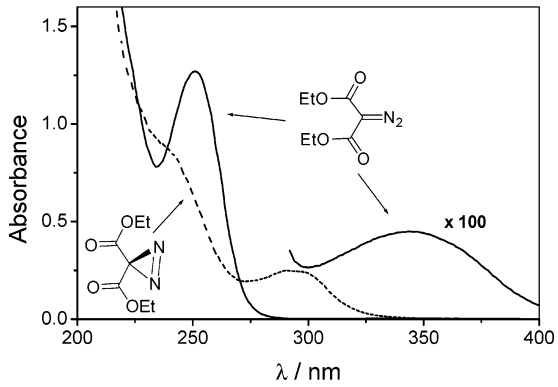

Figure 4. UV spectra of ca. 0.00015 M solutions of ethyl diazomalonate (**1**, −) and of ca. 0.003 M solutions of ethyl 3*H*-diazirine-3,3-dicarboxylate (**2**, - - -) in methanol.

It is interesting to note that the activation parameters for the decomposition of bis-carboethoxydiazirine (**2**) in dioxane are almost identical to the values reported for the cyclic diazirino Meldrum's acid (**4**, $\Delta H^{‡} = 22.2$ kcal M^{-1} and $\Delta S^{‡} = -10.2 \pm 2.4$ cal M^{-1} K^{-1}).[12] In aqueous solution, the situation is drastically different: enthalpy of activation for the decomposition of acyclic diazirine **2** is very close to the dioxane value, while cyclic diazirine **4** decays in water with a substantially lower $\Delta H^{‡} = 12.6$ kcal M^{-1}. This difference can be explained by the different polarity of transition states for the reactions of **2** and **4**. The latter undergoes isomerization from nonpolar diazirine to a very polar diazodicarbonyl compound **3**. The transition state for this process is, therefore, more polar than reagent and is better stabilized by a polar solvent. Ethyl 3,3-diazirinedicarboxylate (**2**), on the other hand, loses nitrogen to produce carbene **5**, which has a polarity similar to the starting material. Thus, the dipole moment of the most stable rotamer of diazirine **2′** is 2.34 D, which is exactly the same as the dipole moment predicted for the most stable conformer of singlet carbene **5** (vide infra). The changes in polarity of the substrate along the reaction coordinate are small, and the enthalpy of activation should be less dependent on solvent polarity.

Photochemistry of Ethyl Diazomalonate (1) and Diethyl 3,3-Diazirinedicarboxylate (2). The UV spectrum of diazomalonate **1** has a strong absorbance at 251 nm and a much weaker band at 344 nm (Figure 4). No fluorescence or phosphorescence was detected at room temperature in solutions of **1** using 254

Scheme 4

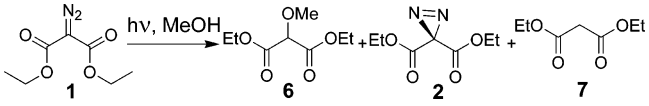

Table 2. Results of Low Conversion Photolyses of Ethyl Diazomalonate (**1**) in Methanol at Different Wavelengths

	wavelength of irradiation λ (nm)				
product	254	300	350	355[a]	sens[b]
	fraction in reaction mixture				
6	0.90	0.83	0.68	0.67	0
2	0.10	0.17	0.32	0.33	0
7	>0.01	>0.01	>0.01	>0.01	1
quantum yield	0.31		0.09		

[a] Monochromatic irradiation using the frequency up-converted output of the Nd:YAG laser. [b] Sensitized photolysis was conducted at 254 nm in 2-propanol using a 10-fold excess of benzophenone as a sensitizer.

and 350 nm excitation light, indicating fast nonradiative depopulation of excited states. The UV spectrum of isomeric diazirine **2** is very different: it shows a weak band at 291 nm and a shoulder on the tail of the short-wavelength band at ca. 244 nm (Figure 4). The spectral characteristics of compounds **1** and **2** are very close to their cyclic counterparts **3** and **4**.[12]

Direct photolysis of the methanol solution of ethyl diazomalonate (**1**) results in the formation of two major products: ethyl 2-methoxymalonate **6**, the product of the O−H insertion reaction of dicarbethoxycarbene (**5**), and diazirine **2**, the product of isomerization of the starting diazo compound (Scheme 4). Trace amounts of ethyl malonate (**7**) were also detected in the reaction mixtures. As was mentioned in the Introduction, the photochemical behavior of the cyclic diazomalonate **3** is very different as it produces mostly Wolff rearrangement products under similar conditions.

The triplet sensitized photolysis of **1** in methanol results in a quantitative formation of the malonic ester (**7**). The triplet reactivity of the diazomalonate **1**, therefore, is similar to that of diazo Meldrum's acid (**3**) and is in line with the accepted mechanism of the photochemical reduction of α-diazocarbonyl compounds through a triplet carbonylcarbene intermediate.[1,2a]

The product ratio of direct photolysis depends on the wavelength of irradiation: shorter wavelengths favor the formation of the O−H insertion product **6**, while isomerization to diazirine **2** becomes a prominent process at $\lambda_{irr} > 300$ nm. Table 2 shows the relative yield of compounds **2**, **6**, and **7** formed in photolysis of ethyl diazomalonate (**1**) at different wavelengths. Product ratios were measured at a low conversion (ca. 10%) to ensure that these values were not affected by secondary photochemistry.

The wavelength dependences of the dediazotization to isomerization product ratio and of the quantum yield are similar to the photochemical behavior of cyclic diazodiester **3**,[12] although they are less pronounced. The short-wavelength irradiation of **1** apparently populates the higher excited state. About one-third of the molecules at this level lose nitrogen to give carbene **5**. The rest of the molecules undergo an internal conversion to S_1, the participation of which is evident from the formation of small amounts of diazirine **2**, and then onto the ground-state surface. The loss of nitrogen from the excited state

Scheme 5

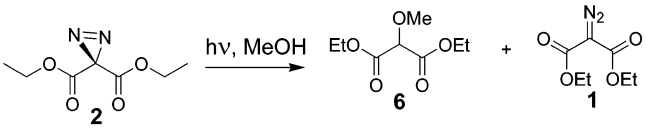

Table 3. Results of Low Conversion Photolyses of Ethyl 3*H*-3,3-Diazirinedicarboxylate (**2**) in Methanol at Different Wavelengths

	wavelength of irradiation (nm)		
product	254	300	350
	fraction in product mixture		
6	0.99	0.81	0.99
1	0.01	0.19	0.01

of diazomalonate **1** should be very fast, in the order of 10^{12} s^{-1}, to compete with the internal conversion. The much higher quantum yield of photolysis at 254 nm than that at 350 nm provides an argument against the formation of a carbene from "hot" S_1 molecules.

Irradiation into a weak long-wavelength band of ethyl diazomalonate results in a higher fraction of molecules populating the lowest excited-state S_1. This state undergoes an efficient thermal deactivation to the ground state, which is evident from a low quantum yield ($\Phi_{350} = 0.09$) of phototransformation of **1** at 350 nm, as well as the absence of fluorescence or phosphorescence of **1**. A small fraction of S_1 population undergoes isomerization into diazirine **2**.

Benzophenone-sensitized photolysis apparently populates the lowest triplet excited state of **1**, which loses nitrogen to produce a triplet carbene $\mathbf{5^T}$. The latter undergoes a double hydrogen abstraction to give ethyl malonate (**7**). Traces of **7** found in direct photolyses are apparently due to the low efficiency intersystem crossing, which yields a triplet excited state of **1**. It is interesting to note that the product of singlet carbene $\mathbf{5^S}$ insertion into the O−H bond of methanol, ethyl 2-methoxymalonate (**6**), was not detected in the triplet-sensitized photolyses of ethyl diazomalonate in methanol. This observation indicates that the abstraction of hydrogen from the solvent by the triplet state of dicarboethoxycarbene ($\mathbf{5^T}$) is much faster than the intersystem crossing to a singlet state.

The photochemical behavior of ethyl 3,3-diazirinedicarboxylate (**2**) is similar to that of its diazo isomer: UV irradiation of **2** results in the formation ethyl 2-methoxymalonate (**6**) accompanied by minor diazirine to diazo isomerization (Scheme 5).

The results of low conversion photolyses (ca. 10%, Table 3) of diazirine **2** allow us to conclude that the O−H insertion product **6** is formed directly from diazirine **2**, rather than from initially formed diazodiester **1**. The molar absorptivity of dicarboethoxydiazirine (**2**) at 300 nm ($\epsilon_{300} = 86$ M^{-1} cm^{-1}) is more than 6 times higher than that of ethyl diazomalonate (**1**, $\epsilon_{300} = 13$ M^{-1} cm^{-1}). Low conversion photolysis of diazirine **2** at this wavelength should not result in the decomposition of the diazo compound formed by isomerization of the starting material. At 254 and 350 nm, the situation is reversed, and a low yield of ethyl diazomalonate is apparently due to secondary photochemistry.

Theoretical Analysis of the Decomposition of Ethyl Diazomalonate (1). The geometries of the structures discussed

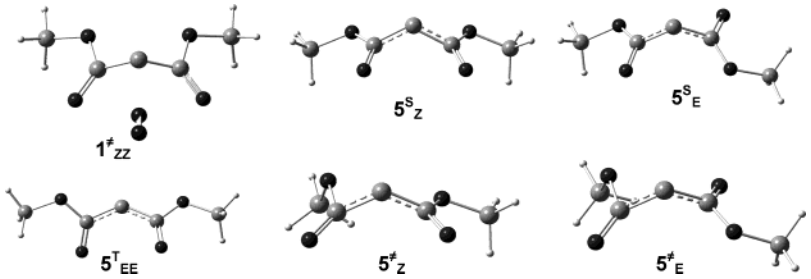

Figure 5. B3LYP/6-311+G(3df,2p) optimized geometries of *syn*-($\mathbf{5^{S}_{Z}}$) and *anti*-($\mathbf{5^{S}_{E}}$) conformers of the singlet carbene, the *E,E* rotamer of a triplet carbene ($\mathbf{5^{T}_{EE}}$), transition states for the dediazotization of *Z,Z*-methyl diazomalonate ($\mathbf{1^{\ddagger}_{ZZ}}$), and for the Wolff rearrangement of the *anti*-($\mathbf{5^{\ddagger}_{E}}$) and *syn*-($\mathbf{5^{\ddagger}_{Z}}$) dicarbomethoxycarbene.

Table 4. Relative Energies and Main Geometrical Parameters of the Equilibrium and Transition Structures Obtained at the B3LYP/6-311+G(3df,2p)//B3LYP/6-311+G(3df,2p) and MP2 (full) aug-cc-pVTZ//B3LYP/6-311+G(3df,2p) (in Parentheses) Levels

	$1^{\ddagger}_{ZZ}$	$1^{\ddagger}_{ZE}$	$1^{\ddagger}_{EE}$	5^{S}_{E}	5^{S}_{Z}	$5^{\ddagger}_{E}$	$5^{\ddagger}_{Z}$	5^{T}_{ZZ}[c]	5^{T}_{ZE}[c]	5^{T}_{EE}[c]
E_{rel}[a,b]	38.8	36.1	35.5	29.5	31.75	37.6	36.7	34.0	32.1	31.0
ZPVE corrected (kcal/mol)				(46.0)	(48.3)	(52.1)	(49.7)	(50.4)	(49.1)	(48.7)
C^1-N^6 distance/Å	2.280	2.200	2.190							
N^6-N^7 distance/Å	1.090	1.090	1.090							
$-\angle C^2C^1C^3$/deg	122.8	125.4	125.1	122.6	123.9	124.0	127.3	143.9	137.0	133.9
$-\angle C^3C^1C^2O^4$/deg	100.5	74.4	65.57	94.9	80.3	82.2	79.8	149.2	−12.5	−31.2
$-\angle C^2C^1C^3O^5$/deg	−100.5	115.9	−65.57	94.9	−80.3	90.8	−90.0	149.1	−130.8	−31.2

[a] Energy difference between $\mathbf{1'_{ZE}}$ and the corresponding structure. [b] Energies of various forms of carbene **5** and transition states $\mathbf{5^{\ddagger}}$ are corrected by the addition of energy of a free nitrogen molecule (−109.5176551 (−109.3936875); ZPVE = 3.513 kcal/mol). [c] Conformations of the triplet dicarbomethoxymethylene are labeled as the conformers of **1′** having similar arrangements of carbon and oxygen atoms in the molecule.

below were preoptimized at the B3LYP/6-31+G(d,p) level and then reoptimized using the extended triple-ζ 6-311+G(3df,2p) basis set. The energies of the resulting structures were also calculated at the full MP2 level using a correlation-consistent Dunning basis set aug-cc-pVTZ.[18] The quantum-mechanical analysis of the mechanism of diazomalonate decomposition is complicated by the presence of several conformations of the species involved.[16] The conformational structure of methyl diazomalonate **1′** and diazirine **2′** is discussed above (Figure 1, Table 1). The electronic energies and representative structural parameters for the *anti*-($\mathbf{5^{S}_{E}}$) and *syn*-($\mathbf{5^{S}_{Z}}$) conformers of the singlet carbene and three rotamers of a triplet carbene ($\mathbf{5^{T}_{ZZ}}$, $\mathbf{5^{T}_{ZE}}$, $\mathbf{5^{T}_{EE}}$), as well as the transition states for deazotization of three conformers of methyl diazomalonate ($\mathbf{1^{\ddagger}_{ZZ}}$, $\mathbf{1^{\ddagger}_{ZE}}$, $\mathbf{1^{\ddagger}_{EE}}$) and the Wolff rearrangement of the *anti*-($\mathbf{5^{\ddagger}_{E}}$) and *syn*-($\mathbf{5^{\ddagger}_{Z}}$) dicarbomethoxycarbene, are summarized in Table 4. The B3LYP/6-311+G(3fd,2p) optimized geometries of $\mathbf{5^{S}_{E}}$, $\mathbf{5^{S}_{Z}}$, $\mathbf{5^{T}_{EE}}$, $\mathbf{1^{\ddagger}_{ZZ}}$, $\mathbf{5^{\ddagger}_{E}}$, and $\mathbf{5^{\ddagger}_{Z}}$ are also shown in Figure 5.

The loss of nitrogen from the methyl diazomalonate (**1′**) results in the formation of a singlet dicarbomethoxycarbene ($\mathbf{5^{S}}$), which exists in two relatively stable conformations with *anti*-($\mathbf{5^{S}_{E}}$) and *syn*-($\mathbf{5^{S}_{Z}}$) orientations of the carbonyl groups (Figure 5). The *anti*-isomer is predicted to be 2.3 kcal/mol lower in energy, and the barrier for the $\mathbf{5^{S}_{E}}$ to $\mathbf{5^{S}_{Z}}$ interconversion is 12.5−13.2 (8.7−9.5) kcal/mol. These results indicate that the rotation of the carbonyl fragment in the singlet dicarbomethoxycarbene $\mathbf{5^{S}}$ is apparently slower than its reaction with methanol, which is known to be a diffusion-controlled process.[14a] Both carbonyl groups in $\mathbf{5^{S}_{E}}$ and $\mathbf{5^{S}_{Z}}$ are almost orthogonal to the plane of the carbene ($C^2-C^1-C^3$, Figure 5). In our opinion, such geometry provides a better overlap of the orbital containing an unshared pair of electrons localized on the carbene atom with the π-system of the carbonyl groups. All three relatively stable rotamers of a triplet dicarbomethoxymethylene ($\mathbf{5^{T}}$), on the other hand, are predicted to be closer to planarity. Similar differences in geometry were reported for the cyclic analogue of **5**,[12] and for acyclic α-carbonylcarbenes.[19] It is interesting to note that both the DFT and the MP2 calculations predict the singlet state ($\mathbf{5^{S}}$) of the dicarbomethoxycarbene to be lower in energy than the triplet ($\mathbf{5^{T}}$), although the energy gap is relatively small (Table 4).

The extrusion of nitrogen from three conformations of diazomalonate **1′** proceeds through three different transition states ($\mathbf{1^{\ddagger}_{ZZ}}$, $\mathbf{1^{\ddagger}_{ZE}}$, and $\mathbf{1^{\ddagger}_{EE}}$) and leads to the formation of a singlet carbene $\mathbf{5^{S}}$ (Table 4, Figure 6). The geometry of the transition state corresponding to the loss of nitrogen from the *Z,Z*-conformer of methyl diazomalonate ($\mathbf{1^{\ddagger}_{ZZ}}$) is shown in Figure 5. It is interesting to note that the C^1-N^6 bond in $\mathbf{1^{\ddagger}_{ZZ}}$ is very long (2.28 Å) and the geometry resembles carbene $\mathbf{5^{S}}$ with a central atom (C^1) located above the plane of the carbonyl groups.

The transition state for the decomposition of the *E,E*-conformer of methyl diazomalonate **1′** has the lowest potential energy. This observation suggests that products produced in the thermal decomposition of acyclic diazomalonates are mostly formed from the *E,E*-conformer. It is interesting to note that the loss of nitrogen from the *E,E*- and *Z,Z*-conformers of **1′** results in the formation of *syn*- dicarbomethoxycarbene ($\mathbf{5^{S}_{Z}}$), while the *Z,E*-conformation produces the *anti*-form of $\mathbf{5^{S}}$.

In contrast with the cyclic diazomalonate **3**,[12] we were unable to locate saddle points on the potential energy surface that connects **1′** with the corresponding ketene, that is, the transition state for the concerted Wolff rearrangement of methyl diazomalonate. The rearrangement of *syn*-($\mathbf{5^{S}_{Z}}$) or *anti*-($\mathbf{5^{S}_{E}}$) dicarbomethoxymethylene to form a ketene, on the other hand, is a

(18) Kendall, R. A.; Dunning, T. H., Jr.; Harrison, R. J. *J. Chem. Phys.* **1992**, *96*, 6796.

(19) Scott, A. P.; Platz, M. S.; Radom, L. *J. Am. Chem. Soc.* **2001**, *123*, 6069 and references therein.

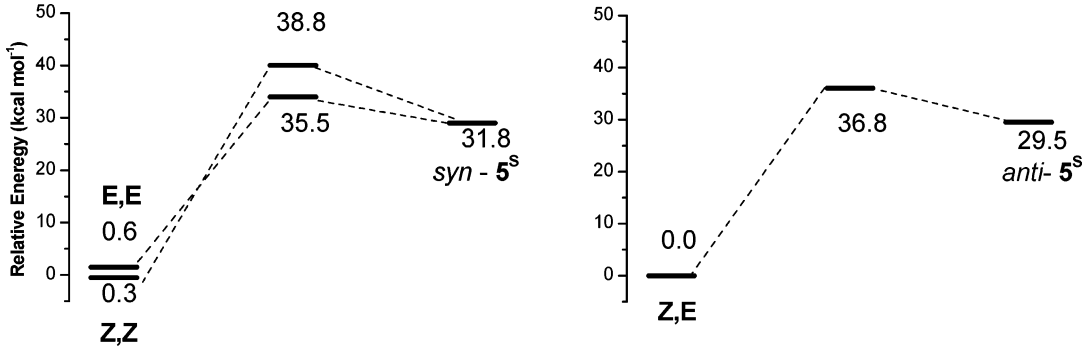

Figure 6. Schematic potential energy profiles for the decomposition of three conformers of methyl diazomalonate **1′**.

feasible process, proceeding via transition states $\mathbf{5}^{\ddagger}_{\mathbf{Z}}$ and $\mathbf{5}^{\ddagger}_{\mathbf{E}}$ correspondingly (Figure 5, Table 4). While a cyclic dicarbalkoxycarbene rearranges to ketene with virtually no activation barrier,[12] the rearrangement of carbene $\mathbf{5}^{\mathbf{S}}$ has a sizable barrier, which is higher for the *anti*-conformer (8.1 (6.1) kcal/mol) than for the *syn*-conformer (5.0 (1.4) kcal/mol). These results agree well with experimental observations on the photochemical reactivity of the ethyl diazomalonate as the photolysis of **1** in methanol solution produces only carbene trapping products. The irradiation of **1′** isolated in a cryogenic matrix, where carbene has nothing to react with, was reported to result in the Wolff rearrangement.[20] It is also interesting to note that barriers for the Wolff rearrangement of $\mathbf{5}^{\mathbf{S}}_{\mathbf{Z}}$ and $\mathbf{5}^{\mathbf{S}}_{\mathbf{E}}$ are lower than the activation barrier for the *syn*- to *anti*-interconversions. In other words, the rearrangement or intramolecular reactions of dicarbomethoxycarbene $\mathbf{5}^{\mathbf{S}}$ are faster than the conformational interconversion.

The Structural Control of the Diazomalonate Reactivity. The photochemically or thermally induced deazotization of the diazo Meldrum's acid (**3**), which is locked in the *Z*,*Z*-conformation, results in a clean Wolff rearrangement via a concerted pathway.[12] The photolysis of the diazirine isomer **4** apparently produces the corresponding α,α-dicarbonylcarbene carbene, which rearranges to the ketene faster than it reacts with the solvent. The photolysis of ethyl diazomalonate (**1**), which also exists predominantly in the *Z*,*Z*-form, results in the formation of carbene **5** and gives no Wolff rearrangement products. The loss of nitrogen from the excited state of **1** is so fast ($k \approx 10^{12}$ s^{-1}) that it does not allow enough time for the conformational changes after the excitation event. The same product (**6**) is formed in the thermal decomposition of **1**, which we believe proceeds mostly through the *E*,*E*-conformation (vide supra). These observations apparently contradict the notion of the conformational control of the reactivity of this class of diazocarbonyl compounds.

To analyze the effect of structural factors on the thermal decomposition of cyclic and acyclic diazomalonates, we have conducted the 2-D relaxed potential energy surface (PES) scans for the decomposition of methyl diazomalonate (**1′**) and diazo Meldrum's acid (**3**). These scans were conducted at the B3LYP/6-31+G(d,p) level of theory in terms of C^1-N^6 and C^1-O^8 (atom migrating in Wolff rearrangement) distances (Figures 7 and 8). The bottom-left corner on the contour plots corresponds to the energy of the starting diazo compound. The extension of the C^1-N^6 bond without explicitly changing the C^1-O^8 distance leads to the formation of the carbene (**5**, bottom-right corner), while the elongation of the C^1-N^6 bond accompanied by the shortening of the C^1-O^8 distance leads to a ketene (upper-right corner).

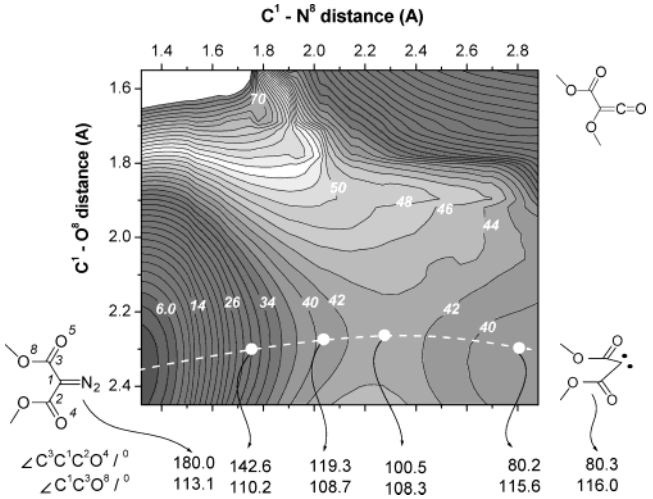

Figure 7. Contour plot of the potential energy surface for the extrusion of nitrogen from the *Z*,*Z*-conformer of methyl diazomalonate **1′**. Values shown on the isoergic lines represent the relative energy in kcal/mol. The values of the $C^3C^1C^2O^4$ dihedral angle and the bond angle of the carbonyl group are shown for representative points on the reaction trajectory.

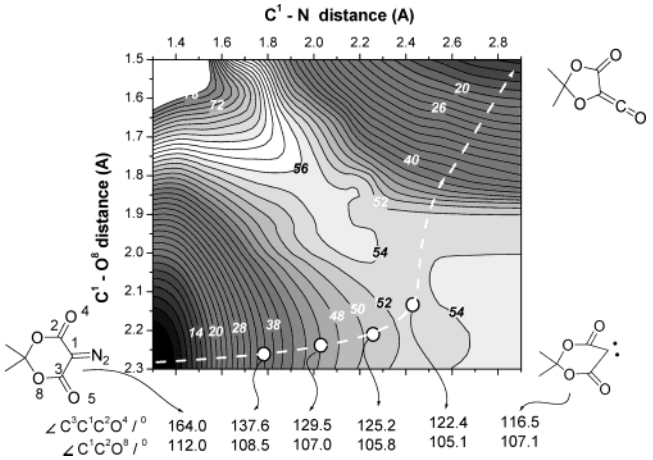

Figure 8. Contour plot of the PES for the Wolff rearrangement of the diazo Meldrum's acid (**3**). Values shown on the isoergic lines represent the relative energy in kcal/mol. The values of the $C^3C^1C^2O^4$ dihedral angle and the bond angle of the carbonyl groups are shown for representative points on the reaction trajectory.

The PES plot for the decomposition of **1′**, shown in the Figure 7, allows us to conclude that the concerted Wolff rearrangement

(20) Visser, P.; Zuhse, R.; Wong, M. W.; Wentrup, C. *J. Am. Chem. Soc.* **1996**, *118*, 12598. McCluskey, A.; Dunkin, I. R. *Aust. J. Chem.* **1995**, *48*, 1107.

is an unfavorable process for this substrate as the synchronous cleavage of the C−N bond and the migration of the methoxy group result in a steep rise in energy. The valley on the PES follows the elongation of the C^1-N^6 bond, eventually reaching the energy plateau at ca. 2.3 Å. At this point, there is a substantial downhill gradient leading the system toward the formation of a carbene $\mathbf{5^S}$, while the migration of the substituent is still an uphill process. This shape of PES explains our failure to locate the transition state for the concerted Wolff rearrangement of **1′** using various algorithms.

The elongation of the C^1-N^6 bond is accompanied by substantial changes in the geometry of the molecule, as the carbon atom of diazo group (C^1) moves out of the plane of two carbonyl groups. These changes are illustrated in Figure 7 by the $C^3C^1C^2O^4$ dihedral angles for several representative structures along the reaction path. The highest point of this path corresponds to the transition state $\mathbf{1^{\ddagger}_{ZZ}}$ (Figure 5). The $C^2-C^1-C^3$ plane in this structure is almost orthogonal to the plane of carbonyl groups, resembling the geometry of the singlet carbene $\mathbf{5^S_Z}$ (Table 4, Figure 5). The bond angle of the carbonyl groups is also getting smaller with the increased C−N distance (Figure 7). This change results in a slight shortening in the distance between C^1 and the oxygen atoms of methoxy groups. The carbonyl bond angle, however, relaxes back to ca. 116° after passing the saddle point. This observation apparently indicates that the oxygen atoms of methoxy groups, while not migrating themselves, still provide some level of anchimeric assistance for the extrusion of nitrogen.

The landscape of PES surrounding diazo Meldrum's acid (**3**, Figure 8) is very similar to that of methyl diazomalonate (**1′**, Figure 7). In fact, the synchronous cleavage of the C−N bond as well as the migration of the substituent is still an unfavorable process as it is characterized by a sharp uphill energy gradient. The extrusion of nitrogen from **3** initially proceeds by the elongation of the C^1-N bond, while the C^1-O^8 distance remains virtually unchanged. This process is also accompanied by the shift of the carbon atom of the diazogroup (C^1) up from the plane of carbonyl groups. The energy plateau is reached at a C^1-N distance of ca. 2.45 Å. The structure corresponding to this point is very close to the one calculated previously for the concerted Wolff rearrangement transition state of **3** and resembles the boat-shaped geometry of the singlet carbene.[12] The gradients felt by the system on this energy plateau, however, are very different from the methyl diazomalonate (**1′**) case. The further elongation of the C^1-N bond leading to the carbene formation is still an uphill process. The migration of the oxygen atom O,[8] on the other hand, has a negative energy gradient, and the system collapses to ketene without formation of a carbene intermediate.

Comparison of the PES plots for the dediazotization of methyl diazomalonate (**1′**, Figure 7) and diazo Meldrum's (**3**, Figure 8) allows us to suggest an explanation for the difference in the reactivity of these two compounds. Both processes start by the extension of the C^1-N bond accompanied by the out-of-plane shift of C^1 until the system reaches the energy plateau at a C^1-N distance in the range of 2.3−2.45 Å. The direction of further transformation, the formation of a carbene versus concerted Wolff rearrangement, depends on the relative stability of the corresponding dicarbalkoxycarbene. The acyclic carbene $\mathbf{5^S_Z}$ can adopt the favorable orthogonal conformation, which results in a relatively deep energy well for these species (ca. 7 kcal mol^{-1}, Table 4). The elongation of the C^1-N bond beyond 2.3 Å in methyl diazomalonate **1′** is, therefore, accompanied by an increase of the dihedral angle between the $C^3C^1C^2$ plane and the planes of the carbonyl group and results in an energy reduction, leading the system to the formation of a carbene (Figure 7).

In the case of a cyclic diazomalonate **3**, this orthogonal geometry and resulting stabilization cannot be achieved, and the energy well corresponding to the cyclic dicarbalkoxycarbene is very shallow (<1 kcal/mol).[12] As a result, the elongation of the C^1-N bond beyond 2.45 Å requires additional energy, while the migration of a substituent from that point on PES is an exoergic process. In other words, diazo Meldrum's acid (**3**) is predicted to undergo a concerted Wolff rearrangement.

Singlet−Triplet Equilibrium of Dicarboethoxycarbene 5. The thermolysis or direct photolyses of ethyl diazomalonates (**1**) and diazirine **2** produce no, or minor traces of, ethyl malonate (**7**). The triplet-sensitized irradiation of ethyl diazomalonate (**1**), on the other hand, results in a quantitative formation of **7**. These observations indicate that a singlet−triplet equilibration of dicarbomethoxycarbene **5** is substantially slower than the intermolecular reactions of the respective states. The singlet carbene $\mathbf{5^S}$ reacts with methanol at 1.5×10^9 s^{-1} M^{-1}.[14a] This value allows us to estimate the lower limit for the activation energy of $\mathbf{5^S \rightarrow 5^T}$ intersystem crossing (ISC) at 4−5 kcal/mol. The rate of the hydrogen abstraction by triplet carbenes from methanol is usually in the order of $1-5 \times 10^6$ M^{-1} s^{-1}, which puts the barrier for the reverse ISC ($\mathbf{5^T \rightarrow 5^S}$) in the range of at least 6−7 kcal/mol.

The substantial height of the ISC barriers of **5** can be explained by the necessity for geometrical changes accompanying the singlet to triplet interconversions. Carbonyl groups in major rotameric forms of the triplet carbene ($\mathbf{5^T}$) are almost coplanar with the carbene ($C^2C^1C^3$ fragment), while the singlet carbene ($\mathbf{5^S}$) has orthogonal geometry (vide supra). We scanned the conformational energy surface of $\mathbf{5^S}$ and $\mathbf{5^T}$ in a search for the intersection. This was done by stepwise changing the geometry of the singlet carbene $\mathbf{5^S_Z}$ from orthogonal to planar and by rotating the carbonyl fragments in $\mathbf{5^T_{EE}}$ and $\mathbf{5^T_{ZE}}$ to the orthogonal geometry of a singlet carbene. The dihedral angles between carbonyl groups and the carbene plane were fixed in steps, while the other degrees of freedom were fully optimized at the B3LYP/6-31+G(d,p) level. The results of these scans are presented in Figure 9.

The energy of the triplet dicarbomethoxycarbene (triangles for $\mathbf{5^T_{EE}}$ and hexagons for $\mathbf{5^T_{ZE}}$, Figure 9) is substantially less dependent on the geometry than the energy of the singlet carbene (circles, Figure 9). The intersections between singlet and triplet surfaces are, therefore, located much closer to the stable conformation of the singlet carbene $\mathbf{5^S_Z}$ than to its triplet form. The analysis of the data represented in Figure 9 allows us to estimate the activation energy of ISC for the *syn*-conformer of the singlet carbene ($\mathbf{5^S_Z}$) at ca. 3 kcal/mol and slightly higher, and at ca. 4 kcal/mol for the *anti*-conformer $\mathbf{5^S_E}$. The activation barrier for the reverse ISC ($\mathbf{5^T \rightarrow 5^S}$) is ca. 4.5−5 kcal/mol. In fact, these estimates of ISC activation barriers should be increased somewhat as we did not take into account another structural parameter, which is different for the $\mathbf{5^S}$ and $\mathbf{5^T}$, the

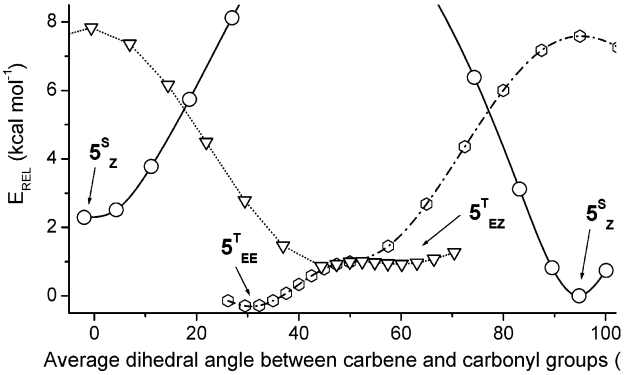

Figure 9. The dependence of the potential energy of the singlet (5^S, circles) and triplet (5^T_{EE}, hexagons; and 5^T_{EZ}, triangles) carbenes on the dihedral angle between the plane of the carbene and carbonyl groups (The energy is plotted versus the averaged value for the $O^4C^2C^1C^3$ and $O^5C^3C^1C^2$ angles.)

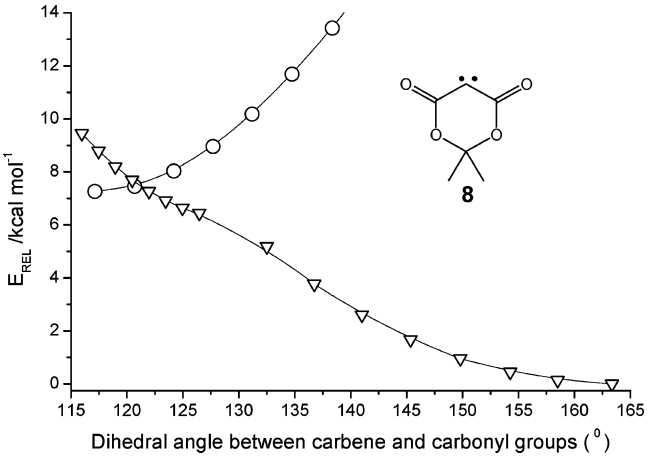

Figure 10. The dependence of the relative energy of the singlet (circles) and triplet (triangles) states of carbene **8** on the dihedral angle between the carbene and carbonyl planes.

bond angle at the carbene carbon (C^1). It is well-known that this angle is larger in a triplet carbene.[2,19]

The direct and sensitized photolysis of a cyclic diazomalonate **3** and its diazirine isomer **4** in methanol also did not produce any evidence of the ISC between the triplet and singlet dicarbalkoxycarbene **8** (Figure 10).[12] Thus, the barrier for the triplet to singlet conversion can be estimated at 6−7 kcal/mol. The quantum-mechanical analysis of this system, in contrast to the dicarbomethoxycarbene (**5**), predicts that the ground state of the carbene **8** is a triplet. The relaxed scan of the PES following the dihedral angle between the carbene plane and the plane of the carbonyl groups in singlet and triplet states of **8** is shown in Figure 10.

The intersection between the triplet and singlet energy surfaces is located very close to the most stable conformation of a singlet carbene **8**, and there is virtually no barrier for ISC to a triplet state (Figure 10). Therefore, the absence of a triplet carbene-derived product in the direct photolysis of **3** provides an additional support for the concerted mechanism of the photo-Wolff reaction of diazo Meldrum's acid (**3**). The reverse triplet to singlet interconversion is predicted to require ca. 7 kcal mol^{-1} of activation energy. This value agrees well with experimental estimates.[12]

Conclusions

The photochemical or thermal decomposition of ethyl diazomalonate (**1**) and ethyl 3,3-diazirinedicarboxylate (**2**) in methanol results in the solvent trapping of dicarboethoxycarbene (**5**). The major conformer of ethyl diazomalonate (**1**) has the same *Z*,*Z*-geometry as its cyclic analogue, diazo Meldrum's acid (**3**). Despite this structural similarity, cyclic diazomalonate **3** shows a very different reactivity, producing Wolff rearrangement products on photolysis in methanol. This observation suggests that ground-state conformation is not the major factor controlling the direction of the decomposition of diazomalonates. DFT analysis of the PES for the loss of nitrogen from cyclic (**3**) and acyclic (**1′**) diazomalonates allows us to conclude that the mechanism of the Wolff rearrangement is controlled by the relative stability of the corresponding carbene, which in turn depends on the rigidity of the molecule. Acyclic carbonyl carbenes adopt a conformation in which the carbonyl group is orthogonal to the carbene plane. This geometry helps reduce the energy of the singlet carbene by conjugative stabilization of its unshared pair. The carbonyl carbene incorporated into a six-membered or a smaller cycle cannot achieve such geometry and is, therefore, unstable directing the Wolff rearrangement into a concerted pathway.

The wavelength dependence of the ethyl diazomalonate photochemistry, as well as the wavelength dependence of the quantum yield, allows us to conclude that the isomerization of diazoester **1** to diazirine **2** takes place from the lowest singlet excited state, while the loss of nitrogen originates from the higher excited state. The rate of the diazo group C−N bond cleavage in the latter should be in the order of 10^{12} s^{-1} to be able to compete with internal conversion.

The singlet dicarbomethoxycarbene (5^S) exists in two relatively stable conformations with *syn*- or *anti*-arrangement of the carbonyl groups. The interconversion between these forms is predicted to be slower than the intermolecular reactions of **5**.

Experimental Section

General Procedures. NMR spectra were recorded on a Varian Unity + 400 MHz or a Varian Gemini 200 MHz spectrometer. All NMR spectra were recorded in $CDCl_3$ and referenced to TMS. The low-temperature NMR experiments were carried out in carbon disulfide containing 20% v/v of $CDCl_3$. FT-IR spectra were recorded on a ThermoNicolet IR200 spectrometer. UV−vis spectra were obtained on a Cary-300 Bio spectrophotometer. Melting points are uncorrected. Purification of products by column chromatography was performed using 40−63 μm silica gel. Tetrahydrofuran was distilled from sodium/benzophenone ketyl; dioxane, ether, and hexanes were distilled from sodium. Ethoxyamine as a free base was obtained by distillation of the corresponding hydrochloride over solid potassium hydroxide at 65 °C. Other reagents were obtained from Aldrich and were used as received unless otherwise noted.

Photolytic Experiments. Analytical photolyses were performed by the irradiation of ca. 10^{-4} M solutions of diazo compound **1** or diazirine **2** in a 1 cm quartz cell using a RMR-600 Rayonet photochemical reactor equipped with a carousel and three sets of eight lamps with λ_{max} values of emission at 254, 300, or 350 nm. Monochromatic irradiations at 355 nm were conducted using a frequency tripled output of a Q-switched Nd:YAG laser. Reaction mixtures were analyzed by HPLC. Pure samples of **1**, **2**, **6**, and ethyl malonate (**7**) were used as references and for calibration of the HPLC detector. Preparative photolyses were conducted by the irradiation of methanolic solutions of ca. 100 mg of substrates using a 16 lamp (with $\lambda_{emission}$ = 254 or 350 nm) Rayonet photochemical reactor and a quartz vessel equipped with an immersible cooling finger. The consumption of starting material was followed by TLC. Determination of a quantum yield was performed using a

ferrioxalate chemical actiniometer.[21] The triplet sensitized photolyses of **1** were conducted using benzophenone as a sensitizer in thoroughly degassed 2-propanol solutions. The concentration of benzophenone was adjusted to achieve a 10 times higher absorbance of the sensitizer than that of the substrate at 254 nm.

Kinetics. Rate measurements were performed using a Carry-300 Bio UV−vis spectrometer equipped with a thermostatable cell holder. Substrate concentrations in the reacting solutions were ca. 10^{-4} M, and the temperature of these solutions was controlled with 0.05 °C accuracy. Reactions were monitored by following the changes in absorbance of ethyl 3*H*-3,3-diazirinedicarboxylate (**2**) at 291 nm. Observed first-order rate constants were calculated by least-squares fitting of a single-exponential function.

Theoretical Procedures. Quantum-mechanical calculations were carried out using the Gaussian 98 program.[22] The levels of theory examined ranged from hybrid B3LYP[23] density functional theory calculations with the 6-311+G(3df,2p)[24] basis sets to the high level composite procedure MP2(full)/aug-cc-pVTZ//B3LYP/6-311+G(3df,2p). For all of the density functional theory calculations, zero-point vibrational energy (ZPVE) corrections, required to correct the raw relative energies to 0 K, were obtained from B3LYP/6-31+G(d,p) method. Analytical second derivatives were computed to confirm each stationary point to be a minimum by yielding zero imaginary vibrational frequencies for the intermediates and one imaginary vibrational frequency for each transition state. These frequency analyses are known to overestimate the magnitude of the vibrational frequencies. Therefore, we scaled the corresponding ZPVE by 0.9772.[25] Initial geometry optimization, IRC calculations for transition states, and relaxed scans of potential energy surfaces were conducted at the B3LYP/6-31+G(d,p) level. In the PES scans, the C^1-O^8 and C^1-N^6 coordinates were fixed in steps, while the other degrees of freedom were fully optimized. Each of the two potential energy surfaces consisted of about 160 points corresponding to different values of C^1-O^8 and C^1-N^6 distances.

Materials. Ethyl diazomalonate (1) was prepared in 64% yield by the diazotransfer reaction[2b] from *N*-*p*-acetamidobenzenesulfonyl azide to ethyl malonate. ^{1}H NMR (200 MHz, $CDCl_3$, δ/ppm): 1.31 (3H, t, $J = 7.4$ Hz), 4.31 (2H, q, $J = 7.4$ Hz). ^{13}C NMR (100 MHz, $CDCl_3$, δ/ppm): 14.29, 61.67, 161.04. IR (neat, cm^{-1}): 2984 (m), 2123 (s), 1758 (s), 1732 (vs). MS/DIP (relative intensity, %): 186 (M^+, 45), 141 (40), 69 (100). UV (MeOH, λ_{max}, nm/log ϵ): 251/3.9, 344/1.34 (lit.[26]).

Ethyl Diazirine-3,3-dicarboxylate (2).[27] Ethoxyamine (0.4 mL, 5.7 mmol) was added dropwise to a stirred solution of ethyl *O*-tosylisonitrosomalonate[28] (660 mg, 1.9 mmol) in 3 mL of acetonitrile under argon at −10 °C over 30 min. After 3 h at this temperature, the reaction mixture was left overnight at 4 °C. The reaction mixture was diluted with 10 mL of ether, and the resulting white crystals were removed. The solvent was removed in a vacuum, and the residue was redissolved in 2 mL of methanol. The colorless crystals of **2** precipitated from methanolic solution at −78 °C and were immediately sublimed at room temperature to give 140 mg (40%) of the desired product. ^{1}H NMR (200 MHz, $CDCl_3$, δ/ppm): 1.30 (3H, t, $J = 7.2$ Hz), 4.26 (4H, q, $J = 7.4$ Hz). ^{13}C NMR (100 MHz, benzene-d_6, δ/ppm): 14.28, 63.16, 163.80. IR (neat, cm^{-1}): 2986 (m), 1755 (s), 1730 (vs). UV (MeOH, λ_{max}, nm/log ϵ): 291/1.94.

Ethyl 2-Methoxymalonate (4). Rhodium tetraacetate (3 mg) was added to a solution of **1** (0.372 g, 2 mmol) in 5 mL of dichloromethane, followed by 0.41 mL (10 mmol) of methanol. The reaction mixture was stirred at 50 °C under an argon atmosphere for 12 h. The solvent was removed, and the reaction mixture was separated on the silica gel column (hexanes:ether, 25:1), giving 370 mg (98%) of **4** as a colorless oil. ^{1}H NMR (200 MHz, $CDCl_3$, δ/ppm): 1.31 (6H, t, $J = 7.4$ Hz), 3.51 (3H, s), 4.31 (4H, q, $J = 7.4$ Hz), 4.41 (1H, s). ^{13}C (100 MHz, $CDCl_3$, δ/ppm): 13.98, 58.58, 61.98, 80.45, 166.25. IR (neat, cm^{-1}): 1739 (vs). MS/DIP (relative intensity, %): 132 (14), 117 (48), 90 (55), 72 (22), 61 (100) (lit.[29]).

Acknowledgment. We are grateful to the National Institutes of Health for partial support of this project (NIH R15 CA91856-01A1). A.B. thanks the McMaster Endowment for a research fellowship.

Supporting Information Available: Tables S1 and S2 of rate data and Gaussian 98 output files for quantum-mechanical calculations. This material is available free of charge via the Internet at http://pubs.acs.org.

JA047824R

(21) Murov, S. L.; Carmichael, I.; Hug, G. L. *Handbook of Photochemistry*; Marcel Dekker: New York, 1993; p 299.
(22) Frisch, M. J.; Trucks, G. W.; Schlegel, H. B.; Scuseria, G. E.; Robb, M. A.; Cheeseman, J. R.; Zakrzewski, V. G.; Montgomery, J. A., Jr.; Stratmann, R. E.; Burant, J. C.; Dapprich, S.; Millam, J. M.; Daniels, A. D.; Kudin, K. N.; Strain, M. C.; Farkas, O.; Tomasi, J.; Barone, V.; Cossi, M.; Cammi, R.; Mennucci, B.; Pomelli, C.; Adamo, C.; Clifford, S.; Ochterski, J.; Petersson, G. A.; Ayala, P. Y.; Cui, Q.; Morokuma, K.; Malick, D. K.; Rabuck, A. D.; Raghavachari, K.; Foresman, J. B.; Cioslowski, J.; Ortiz, J. V.; Stefanov, B. B.; Liu, G.; Liashenko, A.; Piskorz, P.; Komaromi, I.; Gomperts, R.; Martin, R. L.; Fox, D. J.; Keith, T.; Al-Laham, M. A.; Peng, C. Y.; Nanayakkara, A.; Gonzalez, C.; Challacombe, M.; Gill, P. M. W.; Johnson, B. G.; Chen, W.; Wong, M. W.; Andres, J. L.; Head-Gordon, M.; Replogle, E. S.; Pople, J. A. *Gaussian 98*; Gaussian, Inc.: Pittsburgh, PA, 2001.
(23) Becke, A. D. *J. Chem. Phys.* **1993**, *98*, 5648.
(24) Hehre, W. J.; Radom, L.; Schleyer, P. v. R.; Pople, J. A. *Ab Initio Molecular Orbital Theory*; John Wiley & Sons: New York, 1986.
(25) Scott, A. P.; Radom, L. *J. Phys. Chem.* **1996**, *100*, 16502.
(26) Green, G.M.; Peet, N. P.; Metz, W. A. *J. Org. Chem.* **2001**, *66*, 2509.
(27) The procedure we employed for the preparation of diazirine **2** was adopted with some modifications from: Shustov, G. V.; Tavakalyan, N. B.; Pleshkova, A. P.; Kostyanovskii, R. G. *Khim. Geterotsik. Soed.* **1981**, 810.
(28) Biehler, J. M.; Fleury, J. P.; Perchais, J.; Regent, A. *Tetrahedron Lett.* **1968**, 4227.
(29) Hannah, J.; Tolman, R. L.; Karkas, J. D.; Liou, R.; Perry, H. C.; Field, A. K. *J. Heterocycl. Chem.* **1989**, *26*, 1261.